

SUPPORTING INFORMATION

Transverse bacterial migration induced by chemotaxis in a packed column with structured physical heterogeneity

*Meng Wang and Roseanne M. Ford**

Department of Chemical Engineering, University of Virginia, Charlottesville, VA 22904

*Corresponding author phone: (434) 924-6283; fax: (434) 982-2658; e-mail: rmf3f@virginia.edu. Mailing address: Department of Chemical Engineering, University of Virginia, 102 Engineers' Way, P.O. Box 400471, Charlottesville, VA 22904-4741.

I. Hydrodynamic conditions in different structured columns

When considering transport of a solute in a column with two permeable layers parallel to the flow, it was presumed that the solute was diverted into two streams with specific transport characteristics in each layer. According to Darcy's law (1), the velocity in saturated porous media is proportional to the local hydraulic conductivity given a constant hydraulic head. Therefore, the differentiated flow paths aforementioned usually resulted in a solute breakthrough curve with two separate peaks. This phenomenon has previously been reported in Morley's work (2) of studying a column with an inner coarse sand core and an outer fine sand annulus similar to the one used in our study. By pre-inoculating tracer and bacteria in each sand layer before initiating flows in two separate experiments, Morley proved the existence of two distinct flow layers by showing that the elution times for the solute peaks were consistent for pulse injections across the column and for pre-inoculation within each layer.

Table S1: Structure information for different column configurations.

Type	Inner Core (sand/cross area)	Outer Annulus (sand/cross area)	Weighted Breakthrough Volume (mL)	
			Trial A	Trial B
I	Fine (9.08 cm ²)	Coarse (9.02 cm ²)	117.0	118.7
II	Coarse (9.08 cm ²)	Fine (9.02 cm ²)	117.6	107.4
III	Coarse (4.91 cm ²)	Fine (13.19 cm ²)	108.9	108.3
IV	Coarse (2.55 cm ²)	Fine (15.55 cm ²)	108.0	119.4

In our work, we performed tracer tests for a set of heterogeneous columns with different packing structures to further reveal the solute transport patterns in two-layer systems. As indicated in Figure S1, we packed the fine sand in the center and coarse sand

in the surrounding annulus for the Type I column. For the remaining three columns we switched positions of the fine and coarse layers, gradually decreasing the cross-sectional area of the inner layer. Each column had an attractant core along the central longitudinal axis to maintain the same structure as in bacterial experiments. The dimensions of all columns with structured heterogeneity are listed in Table S1.

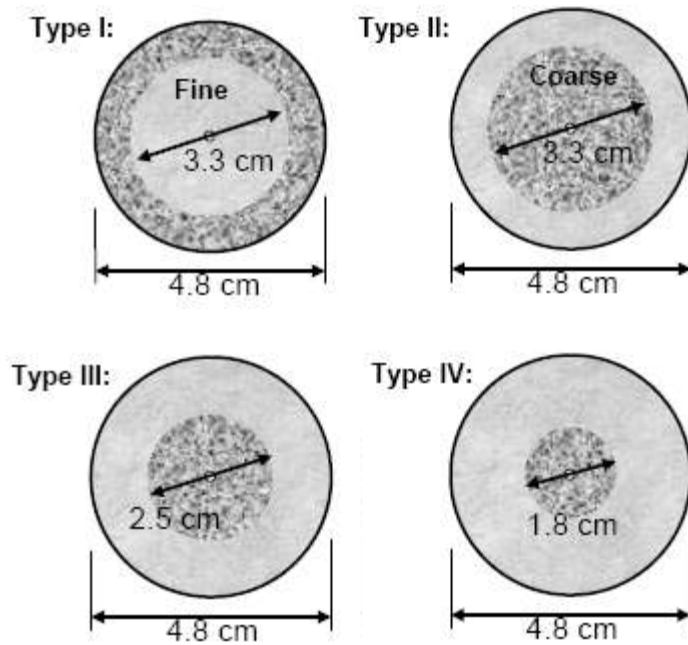


Figure S1: Schematic illustration of structural differences in columns tested for hydrodynamics. The lighter color represents fine sand and the darker color represents coarse sand. The circle at the center represents the attractant core.

The conservative tracer nitrate was injected as a pulse according to the procedures described and its breakthrough was collected for all types of heterogeneous columns under the high flow rate, with a replicate for each case. One group of curves is plotted in Figure S2. Tracer breakthroughs of Type I and Type II had similar configurations. Both of them contained a significant first peak that accounted for >90% of injected mass and an unnoticeable second peak. The similarity might be due to the comparable values of

cross-sectional area for each layer between those two types of columns (Table S1). The area of first peak, which represented the amount of mass transporting through the fast layer, decreased as the cross-sectional area of coarse sand decreased, as illustrated by Type II to IV breakthrough curves. Simultaneously, the growing second peak indicated more solute transporting through the less permeable layer. Despite the significantly different peak distribution for those breakthrough curves from Type I to Type IV, the weighted breakthrough time for all the solute eluted from the column (Table S1) was approximately the same for all the types, equal to one pore volume of the column.

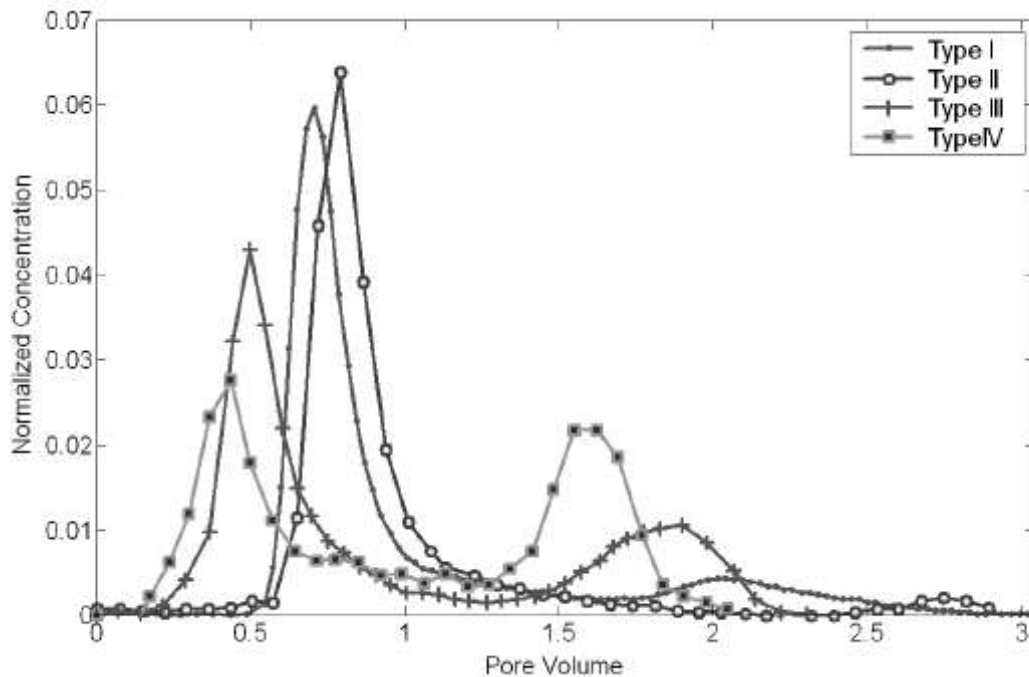


Figure S2: Tracer breakthroughs from different types of columns.

II: Bacterial transport in homogeneous columns

Bacterial transport properties were tested in a column packed with homogeneous sand. The procedure and amount of microbial population injection was kept the same as the heterogeneous ones. The breakthrough curves for strain *E. coli* HCB1 are shown in

Figure S3 and those for *P. putida* F1 and microspheres are presented in Figure S4. Both experimental data and one-dimensional simulation results are plotted.

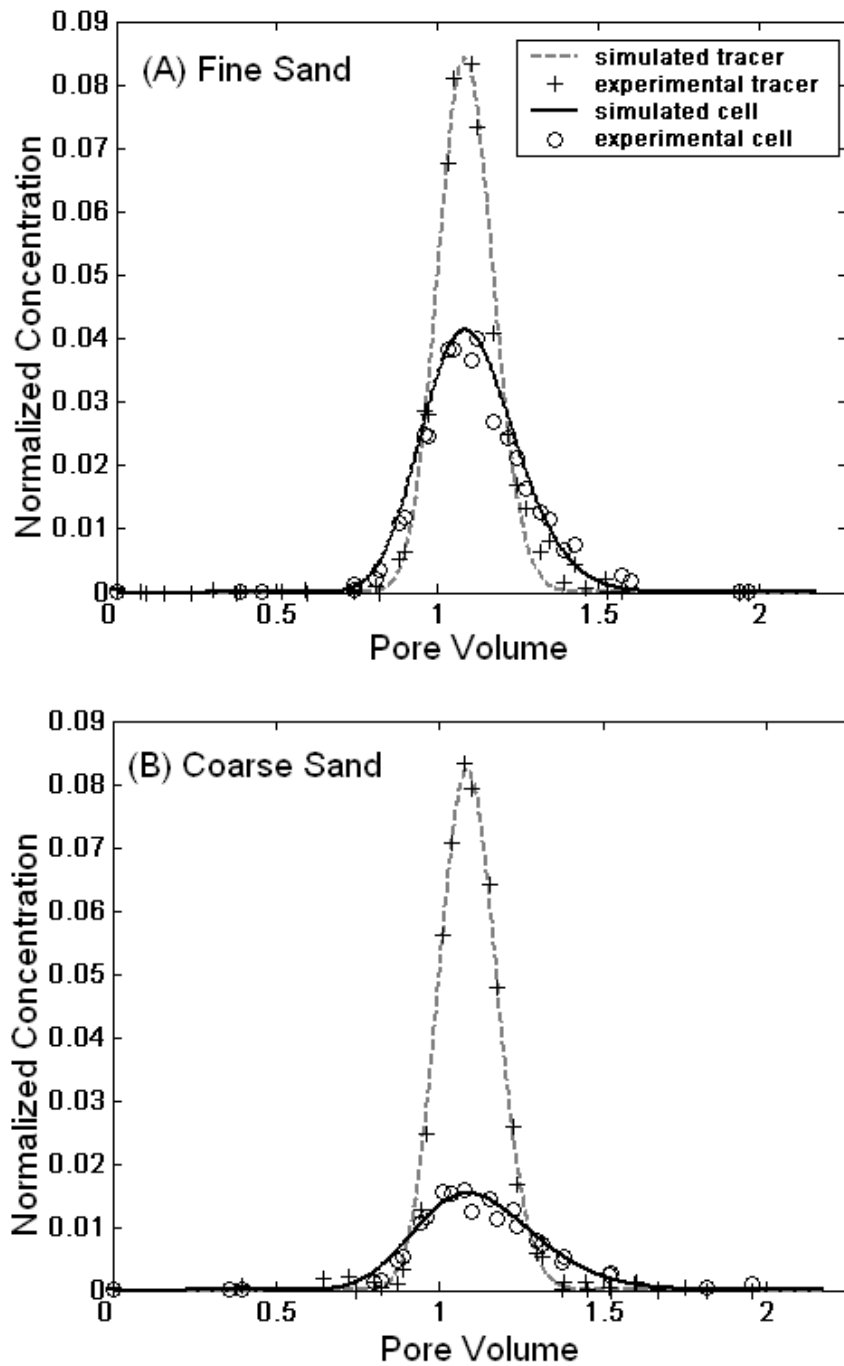


Figure S3: *E. coli* HCB1 BTCs in homogeneous columns under high flow rates with (A) fine sand as the packed material and (B) coarse sand as the packed material. Each trial has a replicate.

Inspection of the data in Figure S3 revealed the difference in adsorption and dispersion properties between *E. coli* and nitrate, and the effects from porous media properties on microbial transport. Relative to approximately 100% recovery of the conservative tracer, *E. coli* cells were found to maintain much lower peak heights in both coarse-grained and fine-grained sand breakthrough curves. As illustrated in Table S2, the mass recovery of *E. coli* was calculated between 75% and 80% in fine sand column studies. In contrast, only about half of the microbial population was recovered through coarse sand. Difference in grain and microbial surface characteristics was hypothesized to cause the discrepancy observed. Additionally, it was noticeably apparent that the longitudinal dispersion of microbes was larger than that of the tracer. The fitted one-dimensional model coefficient values listed in Table S2 supported the observation quantitatively. An approximately 6-fold higher value of the longitudinal dispersivity was required to fit for *E. coli* breakthrough curves compared to the tracer's. Size exclusion effects might cause an early appearance of bacteria in the effluent solutions compared to conservative tracers in porous media (3), and microbial detachment from grains lead to a longer tail of colloids in the breakthrough curves (4). The larger microbial dispersion might be a combined result of those two factors. Additionally, the data in Table S2 showed an increase in dispersion values within larger pore-sized media, as previously recognized (5).

Table S2: Recoveries of tracer, *E. coli*, *P. putida* and microspheres in homogeneous column studies

	Flow Rate (ml/h)	Sand Type	Recovery	
<i>E.coli</i> HCB1	160	Coarse	Trial A	38.57%
			Trial B	39.86%
		Fine	Trial A	75.47%
			Trial B	79.75%
<i>P.putida</i> F1	60	Coarse	Trial A	74.77%
			Trial B	82.61%
		Fine	Trial A	69.00%
			Trial B	75.58%
Microspheres	60	Coarse	Trial A	38.21%
			Trial B	42.11%
		Fine	Trial A	30.29%
			Trial B	28.70%

Table S3: Fitted Parameters of Homogeneous Column Studies of *E. coli* HCB1

	Tracer (Nitrate)		<i>E.coli</i> HCB1	
	Fine Sand	Coarse Sand	Fine Sand	Coarse Sand
Pulse Length(h)	0.033	0.033	0.033	0.033
Pulse Concentration	10 mM	10 mM	5.8E+8 cells/mL	6.9E+8 cells/mL
Flow Velocity (mL/h)	158.7	159.7	158.7	159.7
Porosity	0.42	0.42	0.42	0.42
Dispersion coefficient (cm ² /s)	1.28E-04	1.45E-04	6.46E-04	1.13E-03
Longitude dispersivity (cm)	0.0224	0.0252	0.112	0.196
Retardation Factor (Unitless)	1	1	1.02	1.06
Adsorption coefficient ka (1/h)	0	0	0.26	1.3
Efficiency	98.80%	99.46%	96.65%	95.25%

Note: reported values obtained from average of two trials. Efficiency $E = 1 - \sum(r_i)^2 / \sum(C_i - C_{av})^2$ where r_i is the i th residual between the model observation and the data, C_i is the i th observed concentration, C_{av} is the average of the model observation concentrations. Model efficiencies of 1 indicate a perfect fit.

The apparent differences in adsorption between the two grain-sizes of sand that was observed for *E. coli* was not noticed for *P. putida* according to the breakthrough curves plotted in Figure S4. The recovery of the microorganism in coarse-grained sand, which was approximately 79% as reported in Table S2, was slightly higher than the value 72% obtained in fine-grained sand. The distinct adsorption properties between *E. coli* and *P. putida* were not totally attributed to their different surface characteristics. Given the complicated fluid dynamics in pore spaces under flows, other factors such as bacterial swimming patterns, cell shapes/sizes, and the orientation of microorganisms and grains during deposition were all possible factors that may have contributed to differences in adsorption between those two strains. Breakthrough curves of microspheres were another example to support the importance of colloid physiochemical properties in determining transport fates. Despite having similar effective diameters as *P. putida* cells, microspheres were immotile particles with a different surface chemistry compared to motile bacteria. Those distinctions resulted in a much lower recovery of microspheres than the bacteria, when injected simultaneously.

Similar to the mathematical simulation of *E. coli*, the model captured the experimental observation of *P. putida* well. As demonstrated by the fitted parameters of *P. putida* and microspheres in Table S3, a 2~3 fold higher dispersion coefficient was obtained for bacteria compared with tracers. A similar order of magnitude of increase was also observed for the microspheres. Moreover, the difference in attachment properties was reflected clearly by the change in adsorption coefficients: while this parameter had similar values for *P. putida* in both coarse-grained and fine-grained sands, it was approximately one third of the value for the microspheres.

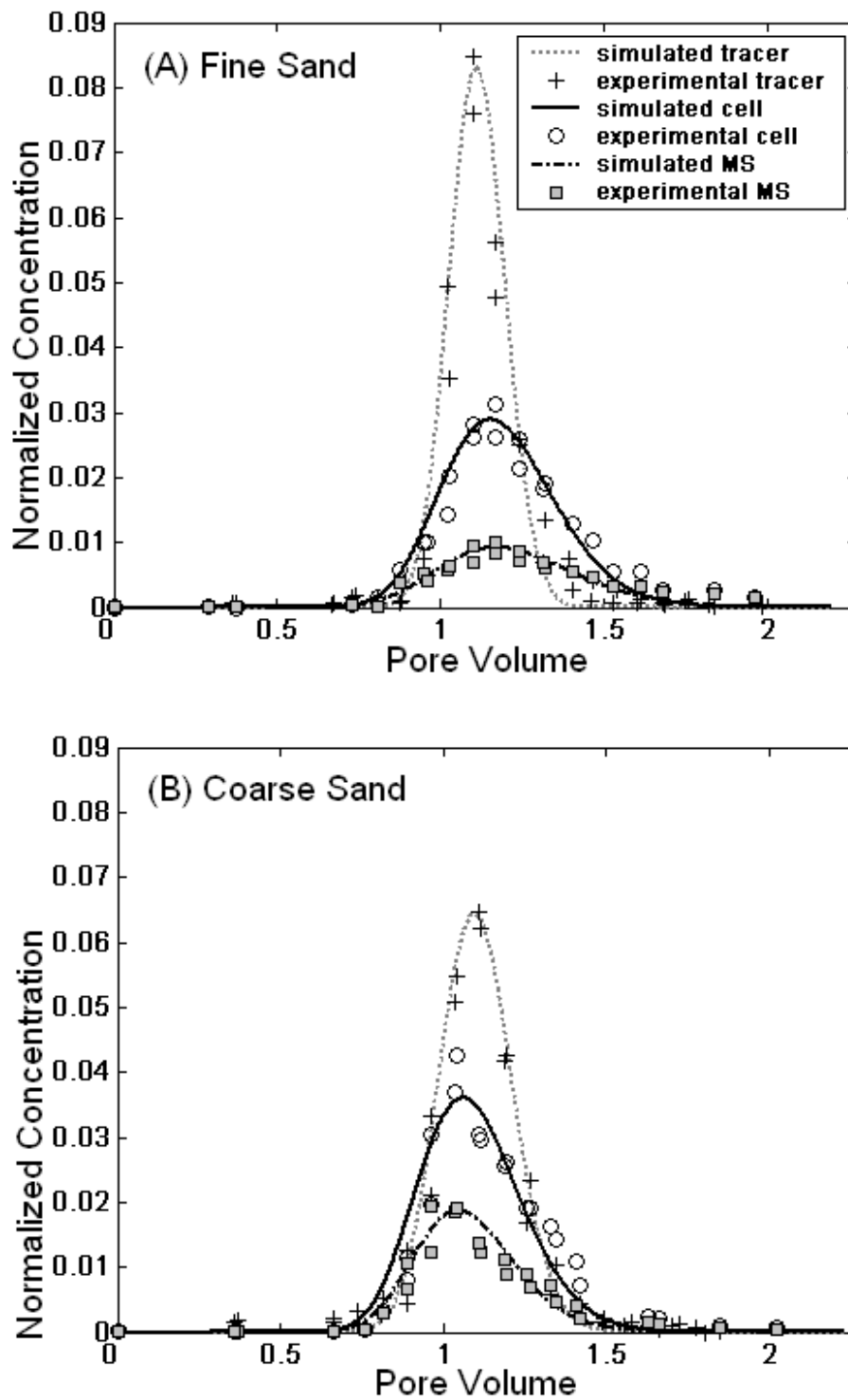


Figure S4: *P. putida* F1 BTCs in homogeneous columns under slow flow rates with (A) fine sand as the packed material and (B) coarse sand as the packed material. Each trial has a replicate. MS represents microspheres.

Table S4: Fitted Parameters of Homogeneous Column Studies of *P. putida* F1

	Tracer (Nitrate)		<i>P. putida</i> F1		Microspheres	
	Fine Sand	Coarse Sand	Fine Sand	Coarse Sand	Fine Sand	Coarse Sand
Pulse Length(h)	0.133	0.133	0.133	0.133	0.133	0.133
Pulse Concentration	10 mM	10 mM	4.0E+8 cells/mL	4.3E+8 cells/mL	1.3E+8 cells/mL	1.5E+8 cells/mL
Flow Velocity (mL/h)	60.35	61.32	60.35	61.32	60.35	61.32
Porosity	0.43	0.43	0.43	0.43	0.43	0.43
Dispersion coefficient (cm ² /s)	7.75E-05	1.51E-04	3.46E-04	3.68E-04	5.07E-04	3.43E-04
Longitude dispersivity (cm)	0.0364	0.07	0.162	0.168	0.238	0.157
Retardation Factor (unitless)	1	1	1.08	0.99	1.15	0.99
Adsorption coefficient ka (1/h)	0	0	0.18	0.13	0.67	0.48
Efficiency	94.63%	97.56%	95.28%	90.52%	90.32%	90.59%

Note: reported values obtained from average of two trials. Efficiency $E = 1 - \sum(r_i)^2 / \sum(C_i - C_{av})^2$ where r_i is the i th residual between the model observation and the data, C_i is the i th observed concentration, C_{av} is the average of the model observation concentrations. Model efficiencies of 1 indicate a perfect fit.

III: Bacterial chemotaxis tests-Agarose Plug Assays

The agarose plug assay is a screening tool to test the chemotactic response of bacteria to a particular attractant. It is also a quick assay to compare the magnitude of chemotactic sensitivity over a range of concentrations (6, 7). As illustrated in Figure S5, an image recorded by a video microscope (Zeiss STEMI SV8) using a 10× objective and a camera (Hamamatsu Orca I), the centered agarose plug contained attractant, which diffused to the ambient environment to form concentration gradients after a bacterial solution was injected into the surrounding space of the chamber. The bacterial population that migrated towards higher attractant concentrations appeared as a white band.

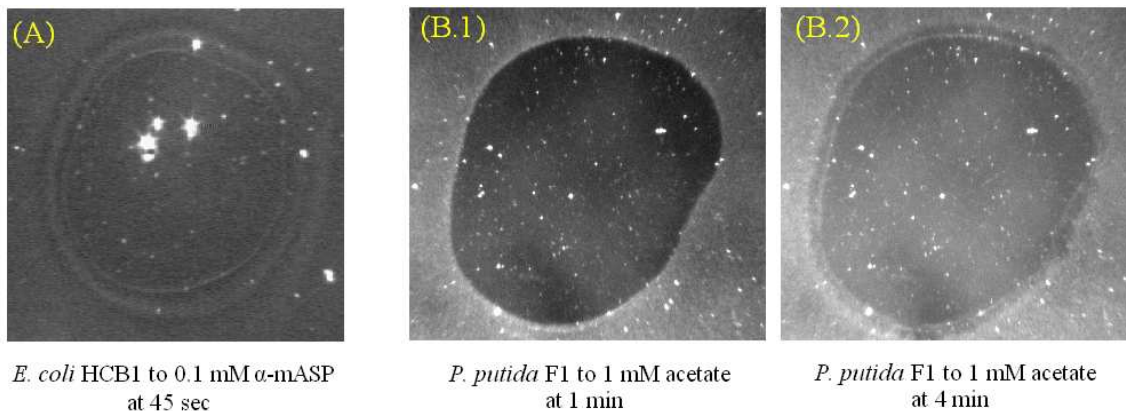


Figure S5. Video images of agarose plug assays to demonstrate chemotactic responses for each strain/attractant pair. (A) *E. coli* HCB1's response to 0.1 mM α -mASP at 45 sec; (B1) *P. putida* F1's response to 1 mM acetate at 1 min. (B2) *P. putida* F1's response to 1 mM acetate at 4 min. The difference of the backgrounds of (B1) and (B2) was due to the different scattering of the light source since the light position was adjusted from image to image in the experiment.

Figure S5 illustrates the results of agarose plug assays for the attractant/bacteria pairs used in our study and indicates the difference in chemotactic response between strains. The white band of *E. coli* in α -mASP plug experiments was apparent within less

than 1 minute as demonstrated in Figure S5-A. In contrast, the response of *P. putida* to acetate was not observable at the same time period (Figure S5-B1) but exhibited a similar white band only after several minutes (Figure S5-B2). The length of time for the chemotactic response correlates with the chemotactic sensitivity for each strain. *E. coli* demonstrated faster and more abundant accumulation in responses to α -mASP while *P. putida*'s band appeared more slowly and was weaker in intensity. The difference in chemotactic strength observed in aqueous solutions may also affect bacterial migration behaviors towards chemical stimuli within porous media.

References:

1. Freeze RA; Cherry, J. A., *Groundwater*. Prentice-Hall: Englewood Cliff, NJ, 1979.
2. Morley, L. Effects of Preferred Flow Path on Transport of Bacteria in Laboratory Columns. Master's thesis, University of Virginia, Charlottesville, VA, 1995.
3. Scheibe, T. D.; Wood, B. D., A particle-based model of size or anion exclusion with application to microbial transport in porous media. *Water Resour. Res.* **2003**, *39*.
4. Camper, A. K.; Hayes, J. T.; Sturman, P. J.; Jones, W. L.; Cunningham, A. B., Effects of Motility and Adsorption Rate Coefficient on Transport of Bacteria through Saturated Porous Media. *Appl. Environ. Microbiol.* **1993**, *59*, 3455-3462.
5. Cussler., E. L., *Diffusion: mass transfer in fluid systems (Second Edition)*. Cambridge University Press, New York, 1997.
6. Parales, R. E.; Ditty, J. L.; Harwood, C. S., Toluene-degrading bacteria are chemotactic towards the environmental pollutants benzene, toluene, and trichloroethylene. *Appl. Environ. Microbiol.* **2000**, *66*, 4098-4104.
7. Toepfer, J. A., The impact of the nucleic acid stain DAPI on the motility and chemotactic behavior of the soil-dwelling bacteria *Pseudomonas putida* F1. Master's thesis, University of Virginia, Charlottesville, VA, 2006.